PNAS RESEARCH ARTICLE | ECOLOGY
ENVIRONMENTAL SCIENCES

# No evidence of canopy-scale leaf thermoregulation to cool leaves below air temperature across a range of forest ecosystems

Christopher J. Still[a,1], Gerald Page[b,c], Bharat Rastogi[d,e], Daniel M. Griffith[a,f], Donald M. Aubrecht[g,h], Youngil Kim[i], Sean P. Burns[j,k], Chad V. Hanson[a], Hyojung Kwon[a], Linnia Hawkins[a], Frederick C. Meinzer[l], Sanna Sevanto[m], Dar Roberts[n], Mike Goulden[o], Stephanie Pau[p], Matteo Detto[q,r], Brent Helliker[s], and Andrew D. Richardson[g,h]

Edited by James Clark, Duke University, Durham, NC; received March 31, 2022; accepted June 28, 2022

**Understanding and predicting the relationship between leaf temperature ($T_{leaf}$) and air temperature ($T_{air}$) is essential for projecting responses to a warming climate, as studies suggest that many forests are near thermal thresholds for carbon uptake. Based on leaf measurements, the limited leaf homeothermy hypothesis argues that daytime $T_{leaf}$ is maintained near photosynthetic temperature optima and below damaging temperature thresholds. Specifically, leaves should cool below $T_{air}$ at higher temperatures (i.e., > ~25–30°C) leading to slopes <1 in $T_{leaf}/T_{air}$ relationships and substantial carbon uptake when leaves are cooler than air. This hypothesis implies that climate warming will be mitigated by a compensatory leaf cooling response. A key uncertainty is understanding whether such thermoregulatory behavior occurs in natural forest canopies. We present an unprecedented set of growing season canopy-level leaf temperature ($T_{can}$) data measured with thermal imaging at multiple well-instrumented forest sites in North and Central America. Our data do not support the limited homeothermy hypothesis: canopy leaves are warmer than air during most of the day and only cool below air in mid to late afternoon, leading to $T_{can}/T_{air}$ slopes >1 and hysteretic behavior. We find that the majority of ecosystem photosynthesis occurs when canopy leaves are warmer than air. Using energy balance and physiological modeling, we show that key leaf traits influence leaf-air coupling and ultimately the $T_{can}/T_{air}$ relationship. Canopy structure also plays an important role in $T_{can}$ dynamics. Future climate warming is likely to lead to even greater $T_{can}$, with attendant impacts on forest carbon cycling and mortality risk.**

leaf temperature | canopy temperature | homeothermy | photosynthesis | leaf traits

## Significance

Leaf temperature has long been recognized as important for plant function, and climate warming may lead to outsized impacts on leaf temperature and function. This includes carbon assimilation, as numerous studies suggest that a variety of ecosystems are operating at or near thermal thresholds. However, sustained, high-frequency measurements of canopy-scale leaf temperature across a range of ecosystems and conditions are rare. We show that daytime canopy leaf temperatures do not cool below air as predicted by the leaf homeothermy hypothesis. Leaves are typically warmer than air and the magnitude of this departure varies with leaf size and canopy structure. Almost all ecosystem photosynthesis occurs when leaf temperature exceeds air temperature. Future warming is unlikely to be mitigated by leaf cooling.

Temperature is a primary environmental control on biological systems and processes at a range of spatial and temporal scales. Its influence spans from enzymatic reactions to ecosystem biogeochemistry to large-scale species distributions. Temperature is also a basic component of climate and much of the concern about the impact of climate warming on the biosphere is motivated by the pervasive influence of temperature on organisms. Leaf temperature ($T_{leaf}$) has long been recognized as important for plant function as it strongly and nonlinearly influences photosynthesis, respiration (1–4), and transpiration (e.g., 5). Dynamics of $T_{leaf}$ in different habitats are also affected by how leaf size varies with climate and latitude. A global meta-analysis of leaf size in relation to environmental variables found that large leaves occur preferentially in warm and wet climates, with $T_{leaf}$ variations affecting selection for maximum possible leaf sizes in differing climates (6). The temperature of leaves is, therefore, of fundamental importance to plant evolution, productivity, and distribution.

There is an emerging appreciation of variation in $T_{leaf}$ and its critical control on many aspects of plant and ecosystem function. Several studies document temperature thresholds for positive net photosynthesis at leaf and canopy scales, with evidence that current temperatures are approaching or surpassing such thresholds, particularly in tropical forests (7–10). This has large implications for forest carbon balance and the global carbon cycle. If tropical canopy photosynthesis declines with increasing temperature while respiration continues to increase, then the strength of the carbon sink in the tropics will be reduced. The temperature sensitivity of leaf respiration—and its acclimation to rising temperature—underlines the importance of accurate $T_{leaf}$ measurements and models for predicting carbon fluxes (4, 11–13). Finally, the increasing prevalence of heat extremes and heat waves resulting from climate warming (14, 15) has heightened interest in how ecosystems respond to such events, in particular, how leaves can avoid heat stress and mortality (16). Thus, understanding $T_{leaf}$ variations and controls

Author contributions: C.J.S., D.M.A., Y.K., S.P.B., C.V.H., H.K., M.G., S.P., M.D., B.H., and A.D.R. collected data; G.P., B.R., D.M.G., D.M.A., Y.K., and S.P.B. prepared data; C.J.S., G.P., B.R., D.M.G., S.P.B., L.H., F.C.M., S.S., D.R., M.G., S.P., M.D., B.H., and A.D.R. analyzed data; C.J.S. wrote the paper; and C.J.S., G.P., B.R., D.M.G., D.M.A., Y.K., S.P.B., C.V.H., H.K., L.H., F.C.M., S.S., D.R., M.G., S.P., M.D., B.H., and A.D.R. assisted with editing the manuscript.

The authors declare no competing interest.

This article is a PNAS Direct Submission.



[1]To whom correspondence may be addressed. Email: chris.still@oregonstate.edu.

This article contains supporting information online at http://www.pnas.org/lookup/suppl/doi:10.1073/pnas.2205682119/-/DCSupplemental.

Published September 12, 2022.

is essential for predicting forest carbon uptake and mortality associated with rising temperatures, heat waves, and droughts.

Based on short-term measurements of $T_{leaf}$ and air temperature ($T_{air}$), Linacre (17) noted that leaves of well-watered plants can deviate from air temperature: leaves were warmer than air below a given temperature and cooler than air above this threshold. Later, Mahan and Upchurch (18) measured $T_{leaf}$ of cotton plants (*Gossypium hirsutum* L.) and highlighted the latter phenomenon, i.e., $T_{leaf}$ was below $T_{air}$ when $T_{air}$ exceeded ~27°C. These observations led to the "limited homeothermy" hypothesis, which posits that leaves cool substantially via transpiration above a threshold $T_{air}$, thus maintaining $T_{leaf}$ closer to optimal values for photosynthesis (18). This hypothesis was expanded by Michaletz et al. (19), who derived a $T_{leaf}/T_{air}$ slope of 0.74 using literature data compiled from many species. In practice, leaf homeothermy—or "leaf homeostasis" (20, 21)—results in slopes <1 when regressing $T_{leaf}$ vs. $T_{air}$ (22). This means that over the course of the day, leaves should warm at a rate slower than the air and, of particular importance, remain cooler than air beyond a threshold temperature, i.e., a negative ($T_{leaf} - T_{air}$) (19, 22). Correspondingly, leaves should experience a narrower range of temperatures than adjacent air if homeothermy is occurring (20). The hypothesis also proposes that transpirational cooling of $T_{leaf}$ will maximize net carbon assimilation, growth, and fitness by maintaining photosynthesis within 90% of optimal rates (19). This implies that significant carbon uptake occurs when leaves are cooler than air (Fig. 1). Finally, if homeothermy is widespread and common, then it should manifest at canopy scales in a range of ecosystems.

It remains unclear whether homeothermy occurs in natural settings (21–24), as well as how $T_{leaf}$ relates to carbon uptake when plants are exposed to large fluctuations of covarying environmental factors. We have a limited appreciation of $T_{leaf}$ regimes in forests and an incomplete understanding of how leaf thermal dynamics upscale to canopy and ecosystem levels (25). Rarer still are datasets that capture simultaneous measurements of the abiotic drivers (e.g., incident solar radiation, wind speed, atmospheric humidity) of $T_{leaf}$ and of ecosystem-atmosphere energy and mass fluxes. This lack of environmental context limits our understanding of canopy $T_{leaf}$ dynamics in response to environmental drivers and hinders our ability to project climate change impacts on forests. Here, we present a multisite synthesis of canopy-scale leaf temperature data—hereafter called canopy-level leaf temperature ($T_{can}$) following (26)—measured at a wide range of forests, including needleleaf-dominated forests, a mixed temperate deciduous broadleaf and evergreen forest, and a tropical broadleaf semideciduous forest. These observations allow us to evaluate $T_{can}$ dynamics at spatial and temporal scales relevant for understanding ecosystem fluxes and climate change feedbacks and fill a critical scale gap between individual leaves and airborne and satellite remote sensing. Canopy-scale temperatures were measured using thermal cameras mounted on towers equipped with eddy covariance systems that measure forest-atmosphere carbon, water, and energy fluxes, along with a suite of environmental variables. Importantly, these measurements spanned multiple seasons and were high frequency (30 min or less) and nearly continuous. With this dataset we assess the limited homeothermy hypothesis and quantify $T_{can}$ and $T_{air}$ patterns. $T_{can}$ patterns are compared with ecosystem carbon fluxes to further test predictions of homeothermy. Finally, we investigate temperature dynamics and drivers at two sites that represent contrasting climate conditions and leaf traits using a theoretical physiological and energy balance analysis.

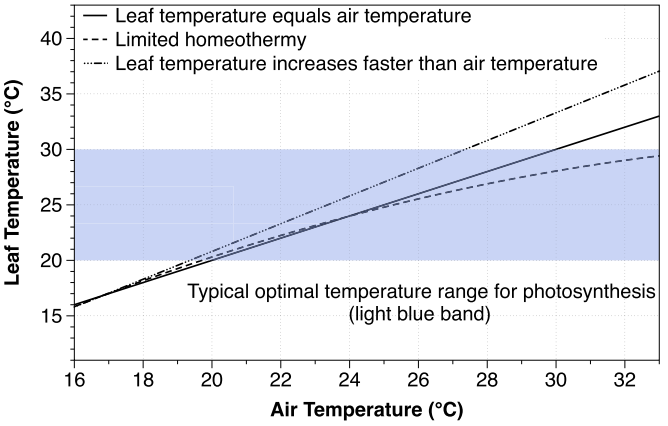


**Fig. 1.** Conceptual model of different $T_{leaf}/T_{air}$ relationships in relation to optimal temperatures for photosynthesis. The solid line is the 1:1 relationship and represents $T_{leaf}$ perfectly coupled to $T_{air}$, while the dashed-dotted line represents a leaf that warms at 1.25 times the rate of air warming. The dashed line represents an example of limited leaf homeothermy where $T_{leaf}$ becomes uncoupled from $T_{air}$ and stays in a narrow optimal temperature range as $T_{air}$ increases, similar to (18). The light blue area represents a typical optimal temperature range for net leaf photosynthesis from (67).

## Results and Discussion

**Observed $T_{can}$ and $T_{air}$ Relationships: Hysteresis and Slopes.** When all available subhourly daytime data (incident shortwave > 25 W $m^{-2}$) were plotted in forests dominated by needleleaf trees (Metolius, Wind River, Pinyon Flat, and Niwot Ridge; Fig. 2) or broadleaf trees (Harvard and Barro Colorado Island [BCI]; Fig. 3), the $T_{can}/T_{air}$ relationships were mostly linear with variations in slope and goodness of fit of a linear regression. The unexplained variation in $T_{can}$ at a given $T_{air}$ was larger at the broadleaf-dominated sites (e.g., BCI adjusted $r^2 = 0.82$) than at the needleleaf-dominated sites (e.g., Wind River adjusted $r^2 = 0.98$). At Harvard Forest where both broadleaf and needleleaf species are present, the $T_{can}/T_{air}$ relationship for regions of interest with needleleaf trees had slightly less scatter (adjusted $r^2 = 0.95$) but a similar slope compared to regions with broadleaf deciduous species (adjusted $r^2 = 0.91$; Figs. 3 *A* and *B*). At all sites, $T_{can}/T_{air}$ slopes were greater than 1 and in most cases well above 1 (using both Model II and ordinary least squares [OLS] regression). Slope values differed little with incident shortwave thresholds varying from 5 to 50 W $m^{-2}$, and $T_{can}$ was usually above $T_{air}$ during the daytime at all sites, with no evidence for a homeothermic cooling at higher temperatures. Canopy leaves also did not experience a narrower range of temperatures than air, as would be expected from homeothermy; indeed, the opposite pattern held at our sites, where leaves were generally colder (nighttime) and warmer (daytime) than air. Importantly, measurements of $T_{air}$ from eddy covariance towers are commonly conducted a few meters above the canopy top. However, $T_{air}$ is well mixed over tall and dense forests because of large and well-developed turbulent structures, especially during daytime with near-neutral and unstable stability conditions (27). This is also confirmed by vertical gradients of $T_{air}$ measured at several of our sites showing small (typically less than 1°C during daytime) differences between the canopy and the tower top, though they can be as large as 2°C at Niwot Ridge (28–30). Thus, observed $T_{can} - T_{air}$ differences were not simply a result of $T_{air}$ being measured above the canopy, but measuring in- and above-canopy $T_{air}$

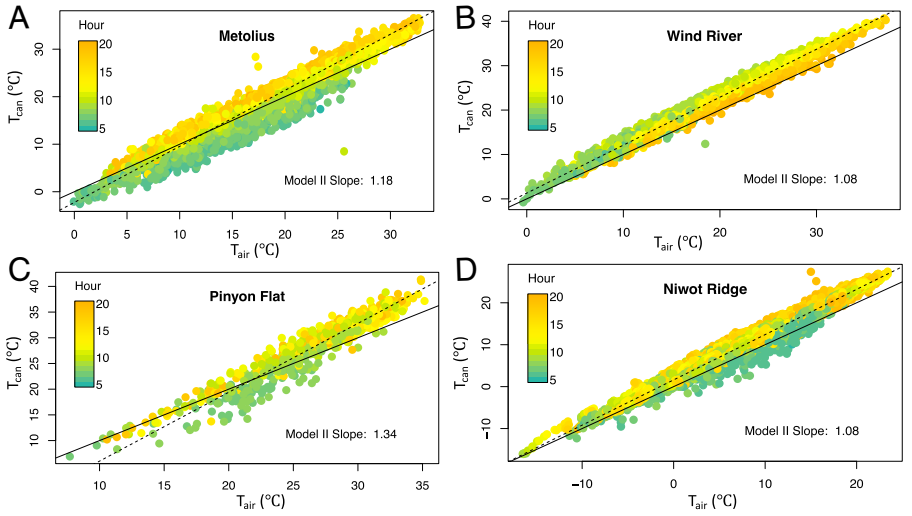


**Fig. 2.** Plots of canopy $T_{can}$ versus $T_{air}$ (both °C) for needleleaf-dominated forest sites (panels *A–D*) in Oregon, Washington, and California. Color shading of symbols is by hour of day. All available values for a single growing season are shown for each site, and only daytime data when downwelling shortwave radiation exceeded 25 W $m^{-2}$ are included. In each panel, the solid line is the 1:1 line and the dashed line and slope are from a model II linear regression using the major axis method calculated using the R package "lmodel2." Regression slopes of $T_{leaf}/T_{air}$ were calculated using Model II major axis regression, as OLS linear regression underestimates the true slope when both variables contain uncertainty.

gradients (e.g., ref. 31) would be an important consideration in future studies.

Throughout an average diel (24-h) cycle during the growing season, canopy leaves of a moist conifer forest (Wind River, WA) warmed faster than air during the morning and cooled faster than air in the late afternoon, leading to a hysteresis and clockwise rotation between $T_{can}$ and $T_{air}$ (*SI Appendix*, Fig. S1). Such hysteretic behavior in the diel hourly mean $T_{can}/T_{air}$ relationships was observed at all sites independent of forest type and climatic characteristics (*SI Appendix*, Fig. S2). Hysteresis was quantified by fitting an ellipse to each dataset and calculating the ratio of the semimajor axis to the semiminor axis, each normalized to the maximum temperatures measured at each site; more circular plots with greater hysteresis have smaller axis ratios. The forests with the smallest hysteresis (i.e., largest axis ratios) were the semiarid pine site (Metolius; *SI Appendix*, Fig. S2*B*) and the arid woodland (Pinyon Flat; *SI Appendix*, Fig. S2*D*) in the western US. These sites have the lowest leaf areas and most open canopies. The sites with the most hysteresis (i.e., lowest axis ratios) were moist temperate or tropical forests at Wind River (*SI Appendix*, Fig. S2*A*), Harvard, MA (*SI Appendix*, Fig. S2*E*), and BCI, Panama (*SI Appendix*, Fig. S2*F*). These sites have closed canopies and the highest leaf area indices; the latter two are dominated by broadleaf species with much larger leaves compared to the other sites.

Multiple interacting biophysical and biological factors can contribute to hysteresis in environmental data (5, 32, 33). Generally, in dense forested areas where soil heating is negligible, the diurnal cycle of canopy warming from absorbed radiation causes the surrounding air to warm up. As warm air mixes up in the surface boundary layer and in the mixed layer above, the planetary boundary layer (PBL) grows, entraining cooler and drier air from above (34). The thermal heat capacity of the forest (primarily heat stored in tree boles) also plays a role, as it

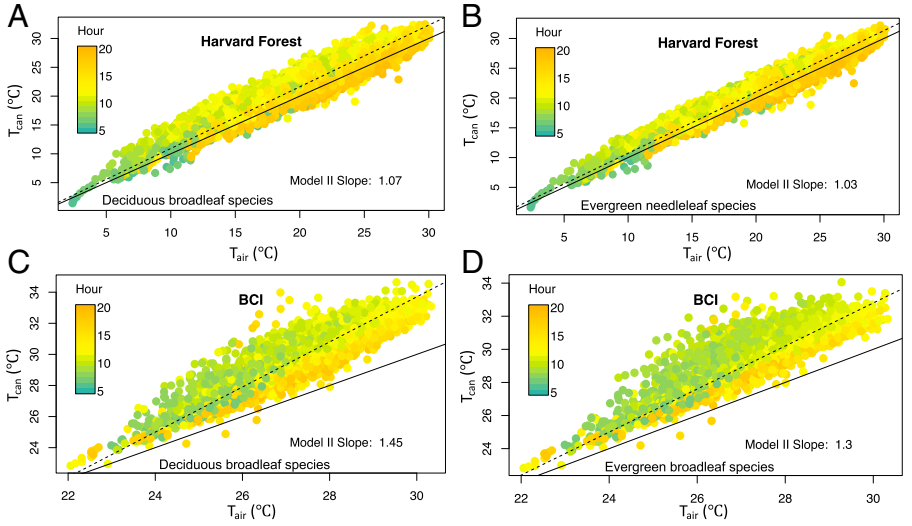


**Fig. 3.** Plots of canopy $T_{can}$ versus $T_{air}$ (both °C) for tree species at Harvard Forest and BCI in Panama. Color shading is by hour of day. Mean values of three broadleaf species (*Acer rubrum*, *Quercus rubra*, and *Betula papyrifera*) at Harvard are shown in (*A*), while one needleleaf species (*Pinus strobus*) is shown in (*B*). Panel (*C*) displays data for deciduous broadleaf species at BCI, while (*D*) is evergreen broadleaf species at this forest site. All available values for the growing season are shown for each species, and only daytime data when downwelling shortwave radiation exceeded 25 W $m^{-2}$ were included. In each panel, the solid line is the 1:1 line and the dashed line and slope are calculated as in Fig. 2.

shifts the peak in surface $T_{air}$ to later in the afternoon (35). Thus, the general $T_{can}/T_{air}$ hysteresis is caused by a combination of surface heating, PBL dynamics, heat capacity, and system inertia, as well as regional processes that affect PBL growth and entrainment. The rotation direction of the hysteresis is related to these dynamics and also to forest structure and climate. Clockwise rotation results when leaves warm faster than air in the morning and stay warmer most of the day, cooling below air late in the afternoon and either staying cooler or remaining near $T_{air}$ throughout the night. The semiarid and arid sites (Metolius and Pinyon Flat) with the least hysteresis were the only ones with anti-clockwise rotation (*SI Appendix*, Figs. S2 *B* and *D*). One possible reason for the anti-clockwise rotation at the semiarid sites is due to the strong nighttime radiative cooling at these sites. This would drive $T_{can}$ well below $T_{air}$, producing a cold memory effect that carries into the morning when leaves remain cooler than air until they are heated by solar radiation. All other sites displayed clockwise rotation, similar to the leaf-scale findings of Gimenez et al. (36). The amount of hysteresis also seems to scale with the canopy aerodynamic conductance to heat and thus to the canopy-air decoupling coefficient, Ω (37, 38). This coefficient varies from 0 (fully coupled) to 1 (fully decoupled) and is affected by wind speed and canopy aerodynamic properties, which together determine surface roughness, along with canopy conductance (*SI Appendix*, Fig. S3). Across sites, the least coupled sites (Harvard, BCI) generally had the most hysteresis (*SI Appendix*, Fig. S2), as well as the most scatter in a linear regression of $T_{can}$ on $T_{air}$ (Fig. 3).

**$T_{can}$-$T_{air}$ Relationships and Ecosystem Fluxes.** Analysis of canopy-scale sensible and latent heat fluxes measured by eddy covariance at these sites provides another assessment of the leaf homeothermy hypothesis. For a forest with a closed energy balance to be consistently colder than surrounding air during daytime, latent heat fluxes have to exceed net radiation ($R_{net}$). Even in the absence of energy balance closure, as is common with eddy covariance measurements (where the sum of sensible, latent, biomass storage terms, and ground heat fluxes is less than $R_{net}$ (39)), sensible heat fluxes would be negative if most canopy leaves were cooler than air. Negative sensible heat fluxes in daytime can occur at canopy scales but typically only in particular conditions such as a rice paddy with an unlimited water supply and surrounded by relatively dry land where evapotranspiration can exceed equilibrium evaporation as a result of the oasis effect (40). Similarly, Blad and Rosenberg (41) showed well-watered alfalfa cooling below air but did not see this same cooling for corn. The only time sensible heat fluxes were negative during the daytime across all of our sites was early in the morning and evening during the day/night transition when photosynthesis was very low (*SI Appendix*, Fig. S4). Sensible heat fluxes can also be used to derive the aerodynamic temperature ($T_{aero}$). $T_{aero}$ is a canopy-scale estimate but is not the same as surface temperature, especially when insolation is high (42, 43). However, as shown in (26) $T_{aero}$ and $T_{can}$ are highly correlated across a range of forest sites. $T_{aero} - T_{air}$ depends on the aerodynamic properties of the canopy (roughness) and the turbulent conditions of the air above the forest. As with $T_{can}$, $T_{aero}$ was typically elevated above $T_{air}$ in the daytime across sites, as was available surface radiometric temperature derived from upwelling longwave fluxes ($T_{LW}$), providing further evidence that canopy-scale leaf homeothermy was not occurring at our sites (*SI Appendix*, Fig. S5).

Understanding how carbon uptake varies with temperature across biomes is a key carbon cycle uncertainty, and it has been argued that homeothermy results from selection for certain leaf traits to optimize instantaneous and lifetime leaf carbon gain (19). Depression of $T_{leaf}$ below $T_{air}$ at higher temperatures should enable higher overall carbon uptake by maintaining leaves within broad optimal photosynthetic temperature ranges and below damaging temperatures (Fig. 1, homeothermy curve). This implies that photosynthesis remains high—and a significant fraction of carbon uptake occurs—when leaves are cooler than air and irradiance is high. At the ecosystem scale, net ecosystem $CO_2$ exchange (NEE) typically increases with daily mean $T_{air}$ until optimal values are reached, beyond which NEE declines with decreasing ecosystem photosynthesis (GPP) and increasing ecosystem respiration (44). The optimal air temperatures for GPP vary broadly across sites in our dataset, from ∼29–31°C at BCI (10) to ∼10–20°C at Wind River (45), Niwot Ridge (46), and at Metolius (25). Thus, if homeothermy were occurring, then we should see depression in $T_{can}$ beyond these broad photosynthetic optima at each site analogous to Fig. 1, but we did not (Figs. 2 and 3). To further assess homeothermy predictions, we explored how GPP was related to $T_{can} - T_{air}$ (Fig. 4). Regardless of forest type, the peak of GPP, and the majority of all carbon assimilation, occurred when canopy leaves were warmer than air at all sites.

A final way to assess the homeothermy hypothesis is to examine the warmest period of each day when the greatest depression in $T_{can}$ relative to $T_{air}$ should occur if homeothermy is happening (Fig. 1). Examination of such conditions at Wind River during the 2015 growing season shows a consistently positive daytime $T_{can} - T_{air}$, and this temperature difference actually increased with $T_{air}$. Additionally, ecosystem fluxes of $CO_2$ and $H_2O$ during the warmest times of day either declined sharply (GPP) or did not change (i.e., latent heat) with increasing maximum $T_{air}$, again counter to expectations from homeothermy (*SI Appendix*, Fig. S6).

**Modeled Canopy-Scale Leaf Temperature: Understanding Abiotic and Biotic Controls on Slope and Hysteresis.** Energy balance modeling (*Materials and Methods*) allows us to illuminate biophysical and biological drivers of the $T_{can}/T_{air}$ relationships in our observations. Multiple micrometeorological variables influence water and energy fluxes and $T_{leaf}$, including incoming $R_{net}$, wind speed, and the vapor pressure deficit (*VPD*). As a first approximation, we adopt a leaf-level approach. We acknowledge the mismatch between this approach and the canopy and ecosystem scale of our temperature and flux measurements, and yet important insights into $T_{can}$ can be gained from such modeling, particularly those features determined by leaf traits, which should be conservative across spatial scales. We focus on a pine forest site (Metolius, OR) and a tropical forest site (BCI, Panama) that represent very different climates and forest types in our dataset (*SI Appendix*, Tables S1 and S2 and Fig. S7). Comparing modeled daytime $T_{leaf}$ to measured daytime $T_{can}$ at both sites revealed reasonable model agreement during representative 6-d summer periods (*SI Appendix*, Fig. S8). The Metolius simulations slightly overpredicted $T_{can}$ at low and underpredicted at high temperatures. The majority of the over- and underpredicted data points occurred in the early morning or evening when the measured leaves stayed cooler or warmer than predictions from either nighttime cooling or daytime heating. At BCI, modeled $T_{leaf}$ closely tracked observed $T_{can}$ but was consistently several degrees cooler.

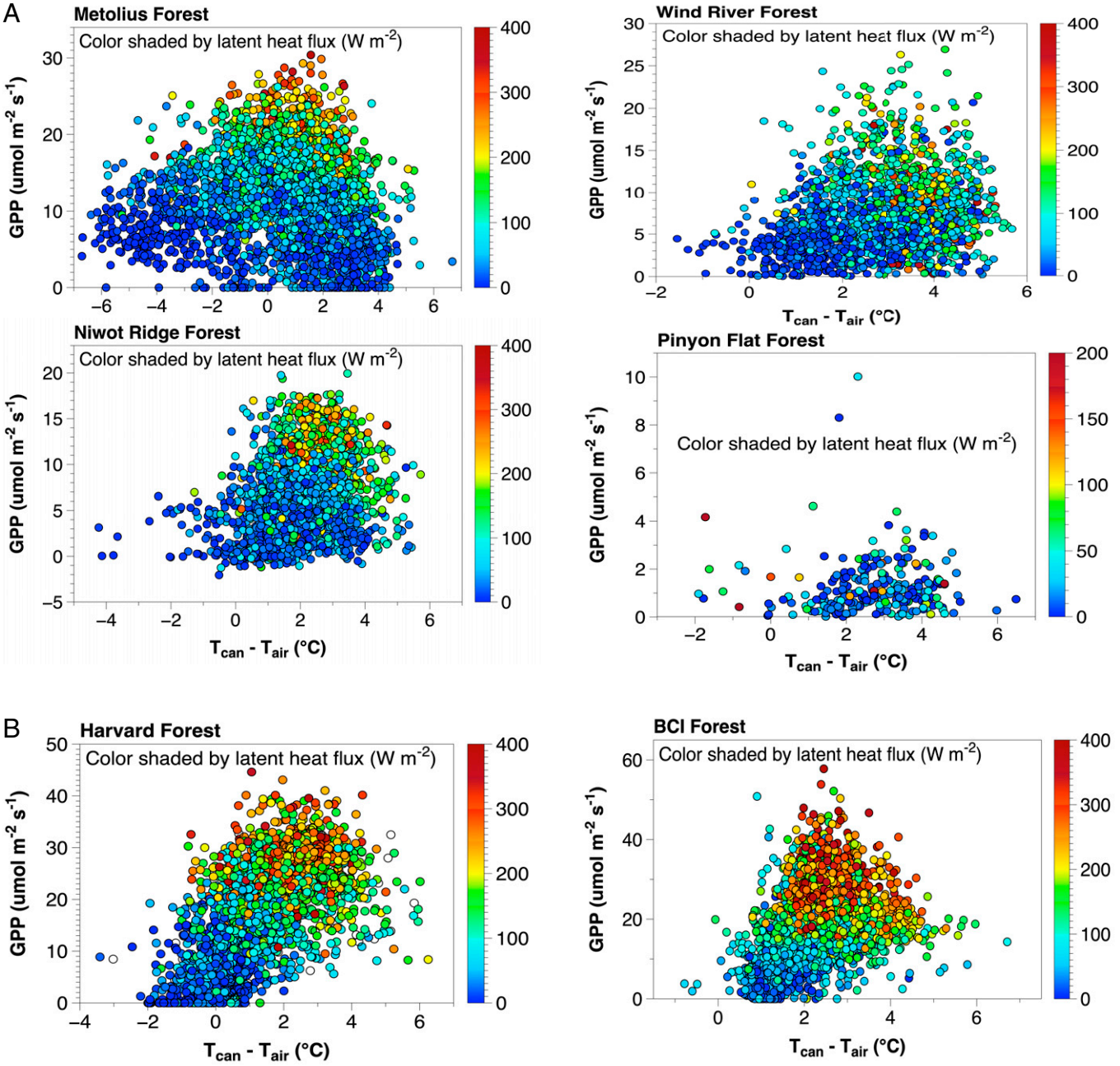


**Fig. 4.** Relationship between gross $CO_2$ uptake (GPP, μmol $m^{-2}$ $s^{-1}$) and $T_{can} - T_{air}$ (°C) at needleleaf-dominated sites (Metolius, Wind River, Pinyon Flat, and Niwot Ridge, *A*) and broadleaf-dominated sites (Harvard, BCI, *B*). The color bar legend represents the latent heat flux (W $m^{-2}$).

Modeling can elucidate how biophysical drivers interact with leaf traits (e.g., leaf size and stomatal conductance to water [$g_s$]) to mediate temperature dynamics. The primary features seen in our $T_{can}$ data across sites ($T_{can}/T_{air}$ hysteresis and slopes >1; *SI Appendix*, Fig. S2 and Fig. 2) were captured by our modeling. Smaller leaves are more efficient in exchanging heat and water vapor because they generate thinner boundary layers at a given windspeed (47) leading to higher boundary layer conductance to heat and water vapor ($g_{bH}$ and $g_{bV}$, respectively). Holding all else constant, as leaf size increases, $g_{bH}$ and $g_{bV}$ decline and the slope and size of the hysteresis of the $T_{leaf}/T_{air}$ relationship increase. In the extreme case of a leaf that only exchanges sensible heat with its surroundings (latent heat = 0), the slope and hysteresis both increase sharply at BCI, but at Metolius only the hysteresis increases. By contrast, at a fixed leaf size, windspeed, and *VPD*, an increase in $g_s$ causes a decrease in the $T_{leaf}/T_{air}$ slope without changing the magnitude of the hysteresis.

Transpiration is not directly controlled by $g_s$, but varies also as a function of leaf size, canopy height and roughness, wind speed, and atmospheric humidity, which determine the boundary layer conductance and stomatal control of transpiration. This variation is captured by the leaf-scale Ω, which depends partly on variables like moisture content and temperature that affect the thermodynamic properties of air. As $T_{air}$ and *VPD* rise, the ratio of $g_b$ to $g_s$ typically increases and Ω decreases for a wide variety of assumed leaf sizes. As a result, as air warms throughout the day, leaves should become *more coupled* to the surrounding air and transpiration will be controlled relatively more by $g_s$ at both sites. The shift in relative control affects not

just the magnitude of transpiration but also its peak timing: stomatally imposed transpiration (i.e., perfectly coupled, $\Omega \geq 0$) tends to peak in the afternoon when *VPD* is highest, whereas equilibrium transpiration (perfectly uncoupled, $\Omega \geq 1$) will peak around solar noon when $R_{net}$ is highest. Our simulations incorporate this leaf-air decoupling, which differs at the two sites: simulated leaves at Metolius were mostly coupled ($\Omega < 0.2$), while those at BCI were more decoupled ($\Omega$ between 0.3 and 0.5). These leaf $\Omega$ ranges are similar to those derived at the canopy scale for these sites (*SI Appendix*, Fig. S3). Leaf coupling differences in our simulations are driven by large differences in leaf size: the leaf characteristic dimension we used for BCI (tropical broadleaf forest) was 10 cm and for Metolius (conifer forest) was 1 cm.

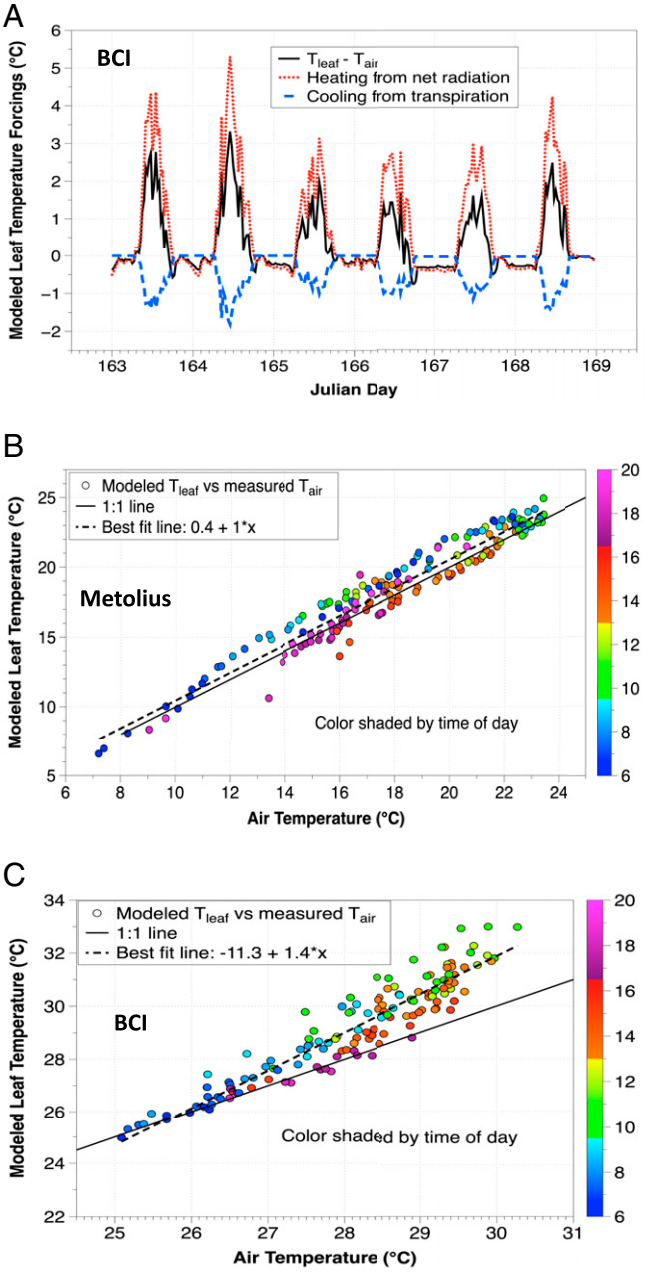


**Fig. 5.** Modeled $T_{leaf} - T_{air}$ (black solid line), leaf heating from $R_{net}$ (W $m^{-2}$, red dotted line), and leaf cooling from transpiration (blue dashed line) at BCI (in °C) shown in (*A*). A typical example of a 6-d summer period for modeled $T_{leaf}$ versus measured $T_{air}$ (both °C) at Metolius (*B*) and BCI (*C*) for representative rain-free periods (May 25–June 1, 2015 and June 12–18, 2015, respectively). Color shading is by hour of day.

Two opposing forces drive the departure of modeled $T_{leaf}$ from $T_{air}$ and thus the slope and hysteresis: heating from incident radiation and cooling from transpiration (Fig. 5*A*). The balance of heating and cooling is modulated by boundary layer conductance. As a typical example at Metolius, modeled daytime $T_{leaf}$ was elevated above $T_{air}$ from midmorning until late afternoon and below $T_{air}$ early in the morning and in the late afternoon and evening (Fig. 5*B*). The morning elevation of $T_{leaf}$ above $T_{air}$ was larger than in the afternoon, resulting from greater radiative heating relative to transpirational cooling. Additionally, windspeeds were lower and less variable in the morning, leading to lower $g_{bH}$ and $g_{bV}$ and greater leaf heating. While modeled $g_s$ at Metolius was relatively high in the morning given typical $g_s$-*VPD* relationships (38, 48), *VPD* was higher in the afternoon (*SI Appendix*, Fig. S7*B*) leading to larger transpiration fluxes. The amount of transpirational cooling with increasing $T_{air}$ depends on whether the relative increase in *VPD* outpaces the relative decline in $g_s$. The relationship between transpiration and *VPD* is often hysteretic, with peaks at intermediate *VPD* values (49–51); additionally, the response of transpiration to increasing *VPD* varies from increasing to decreasing as a function of plant type, photosynthetic pathway, stomatal behavior, and climate (23, 52). Since the increase in *VPD* with $T_{air}$ is well characterized (Clausius-Clapeyron relation), the uncertain response of stomatally imposed transpiration to $T_{air}$ was driven by the sensitivity of $g_s$ to *VPD* and the photosynthetic response to $T_{air}$. If the *VPD* dependence was removed and a fixed $g_s$ was sufficiently large (~0.2 mol $m^{-2}$ $s^{-1}$, or 2–3 times typical maximum values for pines in this ecosystem), then a $T_{leaf}/T_{air}$ slope below 1 would be modeled under conditions of high *VPD*. Thus, it is possible to model homeothermic behavior at Metolius but that would require unrealistic stomatal conductances with no *VPD* feedback.

Our modeling predicts a higher slope and greater hysteresis at BCI than at Metolius (Fig. 5*C*). Transpiration from less-coupled leaves should increase with $T_{air}$ as the fraction of $R_{net}$ that is converted to latent heat increases with $T_{air}$, leading to greater cooling (20). While modeled transpiration was substantial at BCI, it was not large enough to overcome radiative heating (Fig. 5*A*), and so modeled daytime $T_{leaf}$ was elevated above $T_{air}$ with a slope well above 1, again contradicting the homeothermy hypothesis. Modeled $T_{leaf}$ at BCI varied with $\Omega$ (*SI Appendix*, Fig. S9*B*). In nature, the large decoupling of leaves at BCI is likely even more pronounced, as the wind speeds experienced by leaves located within the canopy are even lower than at the canopy top (53, 54). Meinzer et al. (55) calculated $\Omega$ for canopy species in a different Panamanian forest based on wind speeds measured adjacent to leaves; the lower in-canopy wind speeds resulted in $\Omega$ values close to 1. This decoupling likely holds in other tropical forests based on characteristic large leaf sizes and lower in-canopy wind speeds (53, 54, 56). Regardless of the degree of decoupling at BCI, when we simulated $T_{leaf}$ assuming either perfect uncoupling (equilibrium transpiration) or perfect coupling (stomatally imposed transpiration) the $T_{leaf}/T_{air}$ slope was above 1 during this 6-d period. This was due to the inability of the large leaves to shed heat efficiently, with lower maximum $g_{bH}$ than at Metolius.

The discrepancy between our modeling results and the hypothesis of limited homeothermy in (18) can be partly explained by the conditions under which this earlier research was conducted: well-watered crop plants growing in a glasshouse, with high intrinsic $g_s$. They were also growing in isolated pots that likely promoted higher leaf $g_{bH}$ and $g_{bV}$ than would be found in natural canopies (38). Mahan and Upchurch (18) proposed that limited

homeothermy requires three conditions to occur (1): sufficiently large $R_{net}$ (2), abundant soil water to supply high rates of transpiration, and (3) *VPD* gradients large enough to sustain this evaporative cooling. Additionally, energy balance theory predicts that both $g_s$ and $g_b$ must be high for leaves to cool sufficiently to achieve homeothermy (22). These conditions implicitly assume other plant traits that would be required to sustain sufficient transpiration to facilitate homeothermy during hot conditions. These include $g_s$ being largely insensitive to *VPD*, and a plant vascular system with sufficiently high conductivity to sustain substantial transpiration without embolizing. It remains debatable how realistic and common these sets of conditions are for most plants in natural settings. Finally, the inference of homeothermy in leaves appears to depend upon the conditions under which measurements of $T_{leaf}$ and $T_{air}$ are made (i.e., in glasshouses, in gas exchange cuvettes, or in natural settings (57)). Other work with experimentally heated trees finds no evidence for limited homeothermy (21), in agreement with our central finding.

While our results contradict the limited homeothermy hypothesis, leaves can certainly cool below air temperature during daytime, especially in well-watered agricultural plants (17, 18, 40). Plants growing in hot and arid environments also shed heat effectively and can cool below $T_{air}$. Ehleringer et al. (58) documented large temperature depressions in desert leaves due partly to low solar absorptance, while Smith (59) showed substantial depressions of $T_{leaf}$ below $T_{air}$ in large-leaved desert species owing to high transpiration rates. Cook et al. (24) documented homeothermy in well-watered individuals of a desert plant, but not under water-stressed conditions. Dong et al. (20) showed afternoon leaf cooling in several species from a tropical dry woodland while other studies (60, 61) showed how leaf traits like higher reflectance and stomatal density and smaller leaf sizes in plants growing in hot and dry climates enable a greater ability to cool than in plants from warm and humid regions. Finally, shade leaves in high leaf area forests have been shown to remain cooler than or equal to air temperature, while sun leaves are warmer than air (7, 23, 62). Despite these examples, based on our measurements and modeling results, conditions for promoting homeothermy are likely uncommon for sunlit canopy leaves in forested ecosystems. Alternatively, having leaves consistently warmer than air in daytime may even be adaptive in environments where photosynthetic temperature optima are higher than ambient $T_{air}$ (44, 63–66).

Whether and how often leaf homeothermy occurs in natural systems has broad implications for a wide variety of carbon- and water-cycling processes driven by $T_{can}$, especially related to forest responses to climate change. Our results have large implications for understanding plant acclimation to warming, and they suggest a limited ability for canopy leaves to regulate temperature in forest ecosystems. We show that daytime canopy temperatures do not cool below air as predicted by the leaf homeothermy hypothesis. Rather, canopy leaves are typically warmer than air and the magnitude of this departure varies with leaf size and canopy structure. Our data and theoretical analyses suggest that climate warming will lead to even higher canopy leaf temperatures, likely leading to reduction of carbon assimilation capacity and eventually heat damage, as multiple studies suggest that a variety of ecosystems are operating at or near thermal thresholds.

## Materials and Methods

We analyzed thermal images from a range of forest ecosystems to understand how $T_{can}$ varies with $T_{air}$ and with environmental conditions and to provide a test of the limited leaf homeothermy/homeostasis hypothesis. For this analysis, we compiled and present a dataset of $T_{can}$ and environmental variables from a network of forest sites in North and Central America. Importantly, these measurements span multiple growing seasons and are near-continuous in nature, as they were collected by thermal cameras mounted on eddy covariance towers that also measured a wide range of co-located environmental variables, including $T_{air}$, relative humidity, wind speed and direction, short- and longwave radiation, soil moisture and temperature, and ecosystem-atmosphere exchanges of $CO_2$, $H_2O$, and energy. Since we necessarily averaged multiple leaves in each region of interest and then averaged multiple thermal images into hourly data, some extremes in $T_{can}$ are not captured. Thus, the magnitudes of $T_{can} - T_{air}$ reported here are potentially smaller than what individual leaves may experience on shorter time scales. However, our data are more representative of canopy-scale conditions than individual leaf measurements. We also analyzed leaf energy balance equations to provide a theoretical framework for understanding biophysical and physiological factors that regulate $T_{leaf}$ and its interactions with ambient microclimate and radiation. The software R (version 3.5.0) was used for all data preparation and analysis and model simulations; individual packages used are denoted in figure captions.

**Data Availability.** The data for each site have been archived as Rdat files on Zenodo (DOI: 10.5281/zenodo.6862565) (68).

**ACKNOWLEDGMENTS.** C.J.S. acknowledges support from the National Science Foundation (NSF) via the Macrosystems Biology program (EF award 1241953) and the USDA McIntire Stennis program. A.D.R. acknowledges support from the NSF, through the LTER (DEB 1237491, DEB 1832210) and Macrosystems Biology (EF 1241616, EF 1702697) programs. B.H. acknowledges support from the NSF (awards EF 1241873, and IOS 0950998). M.D. thanks BP for its support of Princeton's Carbon Mitigation Initiative. S.S. was supported by Los Alamos Center of Space and Earth Sciences. H.K. and C.V.H. acknowledge support from the US Department of Energy's Office of Science for AmeriFlux core sites. We thank Dave Bowling for providing GPP data for Niwot Ridge.

Author affiliations: [a]Forest Ecosystems and Society, Oregon State University, Corvallis, OR 97331-5752; [b]Biodiversity and Conservation Science, Department of Biodiversity, Conservation and Attractions, Locked Bag 104, Bentley Delivery Centre, Bentley, WA 6983, Australia; [c]CSIRO Land and Water, Private Bag 5, Wembley, WA 6913, Australia; [d]Cooperative Institute for Research in Environmental Sciences, University of Colorado, Boulder, CO 80309; [e]Global Monitoring Laboratory, National Oceanic and Atmospheric Administration, Boulder, CO 80305; [f]Earth and Environmental Sciences, Wesleyan University, Middletown, CT, 06459; [g]Center for Ecosystem Science and Society, Northern Arizona University, Flagstaff, AZ 86011; [h]School of Informatics, Computing, and Cyber Systems, Northern Arizona University, Flagstaff, AZ 86011; [i]Meteorology Section, CFB Trenton, Canadian Forces, ON K8V 5P5, Canada; [j]Department of Geography, University of Colorado, Boulder, CO 80309; [k]National Center for Atmospheric Research, Boulder, CO 80301; [l]USDA Forest Service PNW Research Station, Corvallis, OR 97331; [m]Earth and Environmental Science Division, Los Alamos National Laboratory, Los Alamos, NM 87545; [n]Department of Geography, University of California Santa Barbara, CA 93106; [o]Department of Earth System Science, University of California Irvine, Irvine, CA 92697; [p]Department of Geography, Florida State University, Tallahassee, FL 32305; [q]Department of Ecology and Evolutionary Biology, Princeton University Princeton, NJ 08544; [r]Smithsonian Tropical Research Institute, Balboa 0843-03092, Panama; and [s]Department of Biology, University of Pennsylvania, Philadelphia, PA 19104

1. J. Berry, O. Bjorkman, Photosynthetic response and adaptation to temperature in higher plants. *Annu. Rev. Plant Physiol.* **31**, 491–543 (1980).
2. D. A. Way, W. Yamori, Thermal acclimation of photosynthesis: On the importance of adjusting our definitions and accounting for thermal acclimation of respiration. *Photosynth. Res.* **119**, 89–100 (2014).
3. W. Yamori, K. Hikosaka, D. A. Way, Temperature response of photosynthesis in C3, C4, and CAM plants: Temperature acclimation and temperature adaptation. *Photosynth. Res.* **119**, 101–117 (2014).
4. M. A. Heskel *et al.*, Convergence in the temperature response of leaf respiration across biomes and plant functional types. *Proc. Natl. Acad. Sci. U.S.A.* **113**, 3832–3837 (2016).
5. B. O. Gimenez *et al.*, Species-specific shifts in diurnal sap velocity dynamics and hysteretic behavior of ecophysiological variables during the 2015–2016 el niño event in the amazon forest. *Front. Plant Sci.* **10**, 830 (2019).
6. I. J. Wright *et al.*, Global climatic drivers of leaf size. *Science* **357**, 917–921 (2017).
7. C. E. Doughty, M. L. Goulden, Are tropical forests near a high temperature threshold? *J. Geophys. Res. Biogeosci.* **114**, 1–12 (2009).
8. M. Slot, K. Winter, In situ temperature response of photosynthesis of 42 tree and liana species in the canopy of two Panamanian lowland tropical forests with contrasting rainfall regimes. *New Phytol.* **214**, 1103–1117 (2017).

9. A. C. Mau, S. C. Reed, T. E. Wood, M. A. Cavaleri, Temperate and tropical forest canopies are already functioning beyond their thermal thresholds for photosynthesis. *Forests* **9**, 1–24 (2018).
10. S. Pau, M. Detto, Y. Kim, C. J. Still, Tropical forest temperature thresholds for gross primary productivity. *Ecosphere* **9**, 1–12 (2018).
11. M. Slot, S. J. Wright, K. Kitajima, Foliar respiration and its temperature sensitivity in trees and lianas: In situ measurements in the upper canopy of a tropical forest. *Tree Physiol.* **33**, 505–515 (2013).
12. D. L. Lombardozzi, G. B. Bonan, N. G. Smith, J. S. Dukes, R. A. Fisher, Temperature acclimation of photosynthesis and respiration: A key uncertainty in the carbon cycle-climate feedback. *Geophys. Res. Lett.* **42**, 8624–8631 (2015).
13. J. E. Drake *et al.*, Does physiological acclimation to climate warming stabilize the ratio of canopy respiration to photosynthesis? *New Phytol.* **211**, 850–863 (2016).
14. E. D. Coffel, R. M. Horton, A. de Sherbinin, Temperature and humidity based projections of a rapid rise in global heat stress exposure during the 21st century. *Environ. Res. Lett.* **13**, 014001 (2018).
15. E. Van Gorsel *et al.*, Carbon uptake and water use in woodlands and forests in southern Australia during an extreme heat wave event in the "angry Summer" of 2012/2013. *Biogeosciences* **13**, 5947–5964 (2016).
16. J. E. Drake *et al.*, Trees tolerate an extreme heatwave via sustained transpirational cooling and increased leaf thermal tolerance. *Glob. Change Biol.* **24**, 2390–2402 (2018).
17. E. T. Linacre, A note on a feature of leaf and air temperatures. *Agric. Meteorol.* **1**, 66–72 (1964).
18. J. R. Mahan, D. R. Upchurch, Maintenance of constant leaf temperature by plants–I. Hypothesis-limited homeothermy. *Environ. Exp. Bot.* **28**, 351–357 (1988).
19. S. T. Michaletz *et al.*, The energetic and carbon economic origins of leaf thermoregulation. *Nat. Plants* **2**, 1–9 (2016).
20. N. Dong, I. C. Prentice, S. P. Harrison, Q. H. Song, Y. P. Zhang, Biophysical homoeostasis of leaf temperature: A neglected process for vegetation and land-surface modelling. *Glob. Ecol. Biogeogr.* **26**, 998–1007 (2017).
21. J. E. Drake *et al.*, No evidence of homeostatic regulation of leaf temperature in *Eucalyptus* parramattensis trees: Integration of $CO_2$ flux and oxygen isotope methodologies. *New Phytol.* **228**, 1511–1523 (2020).
22. B. Blonder, S. T. Michaletz, A model for leaf temperature decoupling from air temperature. *Agric. For. Meteorol.* **262**, 354–360 (2018).
23. K. Yi *et al.*, High heterogeneity in canopy temperature among co-occurring tree species in a temperate forest. *J. Geophys. Res. Biogeosci.* **125**, e2020JG005892 (2020).
24. A. M. Cook, N. Berry, K. V. Milner, A. Leigh, Water availability influences thermal safety margins for leaves. *Funct. Ecol.* **35**, 2179–2189 (2021).
25. C. Still *et al.*, Thermal imaging in plant and ecosystem ecology: Applications and challenges. *Ecosphere* **10**, e02768 (2019).
26. C. J. Still *et al.*, Imaging canopy temperature: Shedding (thermal) light on ecosystem processes. *New Phytol.* **230**, 1746–1753 (2021).
27. J. J. Finnigan, R. H. Shaw, E. G. Patton, Turbulence structure above a vegetation canopy. *J. Fluid Mech.* **637**, 387–424 (2009).
28. R. D. Pyles, K. T. Paw, U. M. Falk, Directional wind shear within an old-growth temperate rainforest: Observations and model results. *Agric. For. Meteorol.* **125**, 19–31 (2004).
29. S. P. Burns, P. D. Blanken, A. A. Turnipseed, J. Hu, R. K. Monson, The influence of warm-season precipitation on the diel cycle of the surface energy balance and carbon dioxide at a Colorado subalpine forest site. *Biogeosciences* **12**, 7349–7377 (2015).
30. Y. Kim *et al.*, Canopy skin temperature variations in relation to climate, soil temperature, and carbon flux at a ponderosa pine forest in central Oregon. *Agric. For. Meteorol.* **226**, 161–173 (2016).
31. J. D. Muller, E. Rotenberg, F. Tatarinov, I. Oz, D. Yakir, Evidence for efficient nonevaporative leaf-to-air heat dissipation in a pine forest under drought conditions. *New Phytol.* **232**, 2254–2266 (2021).
32. S. Niu *et al.*, Seasonal hysteresis of net ecosystem exchange in response to temperature change: Patterns and causes. *Glob. Change Biol.* **17**, 3102–3114 (2011).
33. C. Lin *et al.*, Evaluation and mechanism exploration of the diurnal hysteresis of ecosystem fluxes. *Agric. For. Meteorol.* **278**, 107642 (2019).
34. R. B. Stull, *An Introduction to Boundary Layer Meteorology* (Springer Science & Business Media, 1988).
35. S. P. Burns *et al.*, A comparison of the diel cycle of modeled and measured latent heat flux during the warm season in a Colorado subalpine forest. *J. Adv. Model. Earth Syst.* **10**, 617–651 (2018).
36. B. O. Gimenez *et al.*, Species-specific shifts in diurnal sap velocity dynamics and hysteretic behavior of ecophysiological variables during the 2015–2016 El Niño event in the Amazon forest. *Front. Plant Sci.* **10**, 830 (2019).
37. P. G. Jarvis, K. G. Mcnaughton, Stomatal control of transpiration: Scaling up from leaf to region. *Adv. Ecol. Res.* **15**, 1–49 (1986).
38. H. G. Jones, *Plants and Microclimate: A Quantitative Approach to Environmental Plant Physiology* (Cambridge University Press, 2014).
39. K. B. Wilson *et al.*, Energy partitioning between latent and sensible heat flux during the warm season at FLUXNET sites. *Water Resour. Res.* **38**, 30–1–30-11 (2002).
40. D. Baldocchi *et al.*, The impact of expanding flooded land area on the annual evaporation of rice. *Agric. For. Meteorol.* **223**, 181–193 (2016).
41. B. L. Blad, N. J. Rosenberg, Measurement of crop temperature by leaf thermocouple, infrared thermometry and remotely sensed thermal imagery 1. *Agron. J.* **68**, 635–641 (1976).
42. W. P. Kustas, M. C. Anderson, J. M. Norman, F. Li, Utility of radiometric-aerodynamic temperature relations for heat flux estimation. *Boundary-Layer Meteorol.* **122**, 167–187 (2007).
43. K. A. Novick, G. G. Katul, The duality of reforestation impacts on surface and air temperature. *J. Geophys. Res. Biogeosci.* **125**, 1–15 (2020).
44. S. Niu *et al.*, Thermal optimality of net ecosystem exchange of carbon dioxide and underlying mechanisms. *New Phytol.* **194**, 775–783 (2012).
45. Y. Jiang *et al.*, Trends and controls on water-use efficiency of an old-growth coniferous forest in the Pacific Northwest. *Environ. Res. Lett.* **14**, 074029 (2019).
46. T. E. Huxman, A. A. Turnipseed, J. P. Sparks, P. C. Harley, R. K. Monson, Temperature as a control over ecosystem $CO_2$ fluxes in a high-elevation, subalpine forest. *Oecologia* **134**, 537–546 (2003).
47. S. J. Schymanski, D. Or, Wind increases leaf water use efficiency. *Plant Cell Environ.* **39**, 1448–1459 (2016).
48. R. Oren *et al.*, Survey and synthesis of intra- and interspecific variation in stomatal sensitivity to vapour pressure deficit. *Plant Cell Environ.* **22**, 1515–1526 (1999).
49. F. C. Meinzer *et al.*, Atmospheric and hydraulic limitations on transpiration in Brazilian cerrado woody species. *Funct. Ecol.* **13**, 273–282 (1999).
50. M. J. B. Zeppel, B. R. Murray, C. Barton, D. Eamus, Seasonal responses of xylem sap velocity to VPD and solar radiation during drought in a stand of native trees in temperate Australia. *Funct. Plant Biol.* **31**, 461–470 (2004).
51. D. D. Breshears *et al.*, The critical amplifying role of increasing atmospheric moisture demand on tree mortality and associated regional die-off. *Front. Plant Sci.* **4**, 266 (2013).
52. A. Massmann, P. Gentine, C. Lin, When does vapor pressure deficit drive or reduce evapotranspiration? *J. Adv. Model. Earth Syst.* **11**, 3305–3320 (2019).
53. J. Roberts, O. M. Cabral, L. F. De Aguiar, Stomatal and boundary-layer conductances in an amazonian terra firme rain forest. *J. Appl. Ecol.* **27**, 336–353 (1990).
54. S. Fauset *et al.*, Differences in leaf thermoregulation and water use strategies between three co-occurring Atlantic forest tree species. *Plant Cell Environ.* **41**, 1618–1631 (2018).
55. F. C. Meinzer *et al.*, Control of transpiration from the upper canopy of a tropical forest: The role of stomatal, boundary layer and hydraulic architecture components. *Plant Cell Environ.* **20**, 1242–1252 (1997).
56. F. C. Meinzer *et al.*, Environmental and physiological regulation of transpiration in tropical forest gap species: The influence of boundary layer and hydraulic properties. *Oecologia* **101**, 514–522 (1995).
57. C. J. Still, A. Sibley, G. Page, F. C. Meinzer, S. Sevanto, When a cuvette is not a canopy: A caution about measuring leaf temperature during gas exchange measurements. *Agric. For. Meteorol.* **279**, 107737 (2019).
58. J. Ehleringer, O. Björkman, H. A. Mooney, Leaf pubescence: Effects on absorptance and photosynthesis in a desert shrub. *Science* **192**, 376–377 (1976).
59. W. K. Smith, Temperatures of desert plants: another perspective on the adaptability of leaf size. *Science* **201**, 614–616 (1978).
60. H. Lin, Y. Chen, H. Zhang, P. Fu, Z. Fan, Stronger cooling effects of transpiration and leaf physical traits of plants from a hot dry habitat than from a hot wet habitat. *Funct. Ecol.* **31**, 2202–2211 (2017).
61. A. Leigh, S. Sevanto, J. D. Close, A. B. Nicotra, The influence of leaf size and shape on leaf thermal dynamics: Does theory hold up under natural conditions? *Plant Cell Environ.* **40**, 237–248 (2017).
62. B. D. Miller *et al.*, Only sun-lit leaves of the uppermost canopy exceed both air temperature and photosynthetic thermal optima in a wet tropical forest. *Agric. For. Meteorol.* **301–302**, 108347 (2021).
63. W. K. Smith, G. A. Carter, Shoot structural effects on needle temperatures and photosynthesis in conifers. *Am. J. Bot.* **75**, 496–500 (1988).
64. F. Meinzer, G. Goldstein, Some consequences of leaf pubescence in the Andean giant rosette plant *Espeletia timotensis*. *Ecology* **66**, 512–520 (1985).
65. A. P. J. Melcher *et al.*, Determinants of thermal balance in the Hawaiian giant rosette plant, *Argyroxiphium sandwicense*. *Oecologia* **98**, 412–418 (1994).
66. C. Körner, E. Hiltbrunner, The 90 ways to describe plant temperature. *Perspect. Plant Ecol. Evol. Syst.* **30**, 16–21 (2018).
67. D. P. Kumarathunge *et al.*, Acclimation and adaptation components of the temperature dependence of plant photosynthesis at the global scale. *New Phytol.* **222**, 768–784 (2019).
68. C. Still, A. Richardson, M. Goulden, S. Pau, M. Detto, Cross-site Canopy Leaf Temperature and associated Environmental Data. Zenodo. https://zenodo.org/record/6862565. Deposited 19 July 2022.